

SYNTHESIS AND STEREOCHEMISTRY OF BILIRUBIN ANALOGS LACKING CARBOXYLIC ACIDS

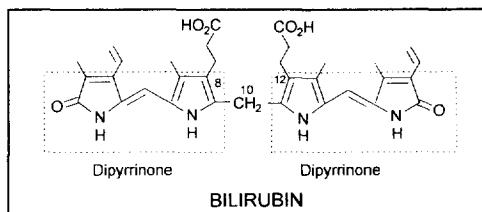
Stefan E. Boiadjev, William P. Pfeiffer and David A. Lightner*

Department of Chemistry, University of Nevada, Reno, Nevada 89557-0020 USA

Abstract: Bilirubin analogs with propionic acid groups replaced by *sec*-butyl (1), 3-acetoxy-1-methylpropyl (2) or 3-acetamido-1-methylpropyl (3) were synthesized in enantiopure form and known absolute configuration. Although there are no propionic acid groups to act in stabilizing folded, ridge-tile conformations, the (*S*) stereogenic centers induce the pigments to adopt a left-handed (*M*) helicity — as evidenced by exciton circular dichroism spectra.
 © 1997 Elsevier Science Ltd.

INTRODUCTION

Bilirubin is a bis-dipyrri-*none* dicarboxylic acid formed in normal human metabolism of heme proteins^{1,2,3} at a rate of ~300 mg/day, mainly from the breakdown of red blood cells. High levels of serum bilirubin, which is lipophilic and intrinsically unexcretable, can cause irreversible neurologic damage. But the pigment is efficiently eliminated by the liver following uptake and enzymic conversion



to water-soluble glucuronides that are promptly secreted into bile. Impaired excretion of the glucuronides occurs in many types of hepatobiliary disease, but retention of native bilirubin is principally observed in newborn babies.¹⁻³ Accumulation of either native bilirubin or its glucuronides in the body is manifested in jaundice.

Bilirubin is conformationally flexible in solution, but one conformation is significantly more stable than all the others: a ridge-tile structure with intramolecular hydrogen bonds between the pyrrole and lactam functions of the dipyrri-*none* halves and the propionic carboxyl (or carboxylate) groups (Fig. 1).^{4,5} It can adopt porphyrin-shaped conformations, but these are disfavored and of relatively high energy. It might also adopt the linear conformation shown above, but it is especially high energy.^{5,6} In fact, the ridge-tile shape is the only one that has been observed in crystals of bilirubin^{4a,b} and its carboxylate salts.^{4c} Spectroscopic studies, particularly NMR,^{7,8,9} supported by energy calculations,^{5a,6} strongly suggest that hydrogen-bonded ridge-tile conformers also prevail in solution. Individual ridge-tile conformers of bilirubin are conformational enantiomers that interconvert rapidly^{7,8} in solution through a succession of non-planar intermediates in which the hydrogen bonding network is never completely broken.^{5a,6} Yet, the energetically most favored ridge-tile conformation (interplanar angle, $\theta \sim 100^\circ$) is *not* rigid. It is flexible; and small, low energy rotations about the C(9)-C(10) and C(10)-C(11) bonds cause θ to close

or open somewhat, while maintaining hydrogen bonding.^{5a,10} Large rotations, of course, close or open the conformation, book-like, breaking hydrogen bonds and leading to energetically disfavored conformations. Such large bond rotations are associated with the interconversion of mirror image ridge-tile conformations, a dynamic process occurring at an experimentally-determined rate of $\sim 5.4 \text{ sec}^{-1}$ at 37°C ⁷ over an experimentally-determined barrier of $\sim 18\text{--}20 \text{ kcal/mole}$.^{7c}

Bilirubin and its analog mesobilirubin-XIII α are thus a 50:50 mixture of equilibrating conformational enantiomers

(Fig. 1), and displacement of the equilibrium toward one or the other of the enantiomers can be achieved by complexation with a chiral compound, such as quinine¹¹ or serum albumin,^{12,13} and observed by circular dichroism (CD) spectroscopy. Selective stabilization of one enantiomer can also be achieved through intramolecular non-bonded steric interactions, as has been observed when stereogenic centers are created by methyl substitution at either the α or the β carbons of the propionic acid chains.⁸ An especially useful allosteric model, ($\beta S, \beta' S$)-dimethylmesobilirubin-XIII α (**22**) has thus been used to probe intramolecular hydrogen bonding and conformational enantiomerism (Fig. 1). It is thought to adopt mainly the *M*-helical ridge-tile conformer in which non-bonded steric interactions are minimized.^{8a} Such "intramolecular resolution," but absent the intramolecular hydrogen bonding, is also the subject of the current work. It occurred to us that the related optically active rubins (**1-3**) might also be used to probe pigment stereochemistry — except in these models there is little (**3**) or no (**1** and **2**) opportunity for intramolecular hydrogen bonding. Yet, if nonbonded steric interactions remain important and if large CD Cotton effects are seen, it would seem likely that an important conformation-determining element in all bilirubins is simply the minimization of nonbonded steric interactions, which favors a ridge-tile shape.^{5,6}

RESULTS AND DISCUSSION

Synthesis. Bilirubin analogs **1-3** were prepared from optically active dipyrinones **7-9**, as outlined in the Synthetic Scheme. Thus, oxidative coupling using *p*-chloranil¹⁴ led to 56-88% yield of verdins **4-6**, which were readily converted to rubins **1-3** in 67-89% yield using sodium borohydride. The optically active dipyrinones (**7-9**) of known absolute configuration were prepared from a common precursor, monopyrrole **14**, which had been synthesized and resolved earlier.^{8a} Conversion of **14** to **7** was achieved following (i) diborane reduction of the CO_2H group to CH_2OH in **13**,¹⁵ (ii) conversion to tosylate **12**,¹⁵ (iii) reaction of the tosylate with Zn and NaI in dimethoxyethane

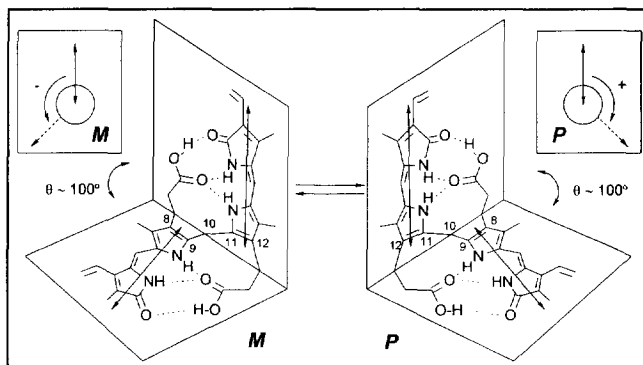
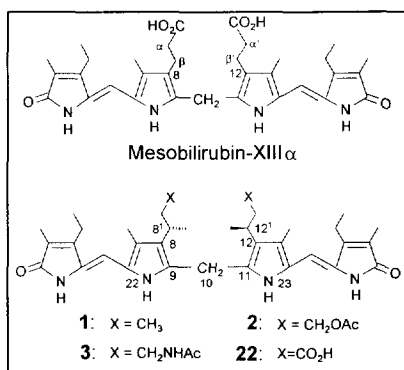
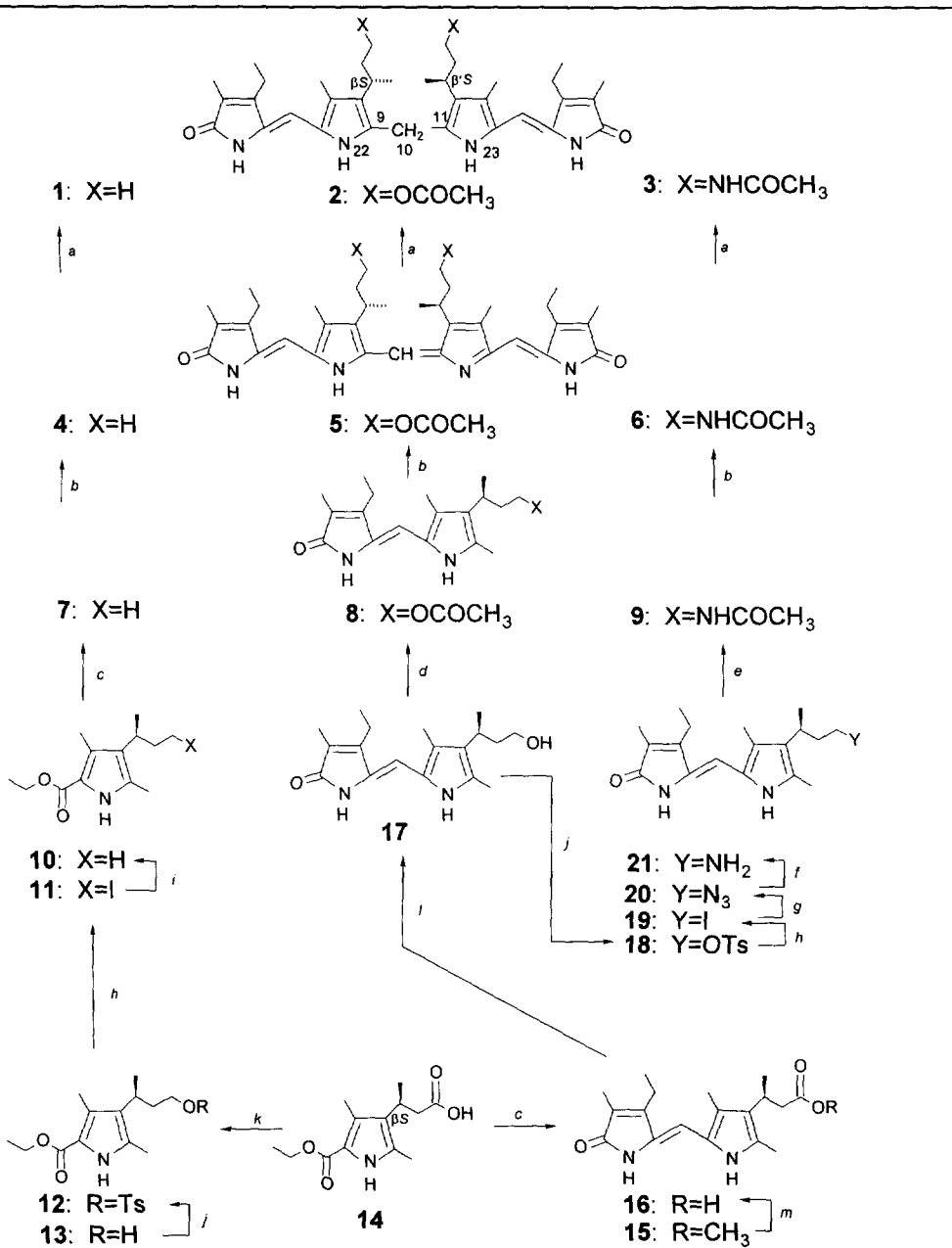


FIGURE 1. Interconverting intramolecularly hydrogen-bonded enantiomeric conformers of bilirubin-IX α . The double headed arrows represent the dipyrinone long wavelength electric transition moments (dipoles). The relative helicities (*M*, minus or *P*, plus) of the vectors are shown (inset) for each enantiomer. Hydrogen bonds are shown by dotted lines.



SYNTHETIC SCHEME



^a NaBH₄, CH₃OH, THF; ^b *p*-chloranil, HCOOH; ^c NaOH, Δ, then HNO₃, then 5-bromomethylene-4-ethyl-3-methyl-2-oxo-1*H*-pyrrole in CH₃OH, Δ; ^d Ac₂O/pyr; ^e AcOH, DCCl, DMAP; ^f φ₃P/THF-H₂O; ^g NaN₃/DMF; ^h NaI/acetone; ⁱ Zn, NaI, DME; ^j TsCl/pyr.; ^k BH₃•THF; ^l CH₃CH₂OCOC/Et₃N-THF, then NaBH₄ at -20°C; ^m NaOH/H₂O, then HCl.

to give **10**, via iodide **11**, and (iv) condensation of saponified **10** with 5-bromomethylene-4-ethyl-3-methyl-2-oxo-1*H*-pyrrole.¹⁶ Dipyrinone **8** was prepared in two steps in 88% yield from known dipyrinone acid **16**:¹⁵ (i) first by reduction of the mixed anhydride of **16** (from ethyl chloroformate) with NaBH₄ in 91% yield, (ii) then esterification of **17** using acetic anhydride in pyridine. Dipyrinone **17** was converted to dipyrinone **9** in 5 steps by the functional group modifications outlined: (i) **17** was converted to its tosylate (**18**) in 79% yield, using *p*-toluenesulfonyl chloride in pyridine; (ii) **18** was converted to its iodide (**19**) in 94% yield with NaI in acetone; (iii) iodide was displaced from **19** using NaN₃ in DMF to afford a 91% yield of azide **20**; (iv) **20** was reduced to the amine with triphenylphosphine-THF-H₂O; and (v) the amine was acetylated *in situ* to form acetamide **9** in 93% yield for both steps using acetic acid, DCC and DMAP. The isolation and purification of amine **21** proved to be difficult; thus it was prepared and acetylated in one pot.

Circular Dichroism and Exciton Coupling. Moderately strong bisignate CD spectra (Fig. 2) were observed in CHCl₃ for **1-3**, which may be viewed as bis-dipyrinones. In clear contrast, the CD spectra of dipyrinones **7-9** are extremely weak at best (Fig. 2, Table 1), in accord with expectations for a $\pi \rightarrow \pi^*$ CD transition perturbed by dissymmetric vicinal action.^{15,17} The few weak bisignate CD spectra found in **7-9** come from dimers^{15,17} formed in nonpolar solvents. The strong bisignate Cotton effects of **1-3** are characteristic of an exciton system in which the two dipyrinone chromophores interact by coupling locally excited $\pi \rightarrow \pi^*$ transitions (electric transition dipole

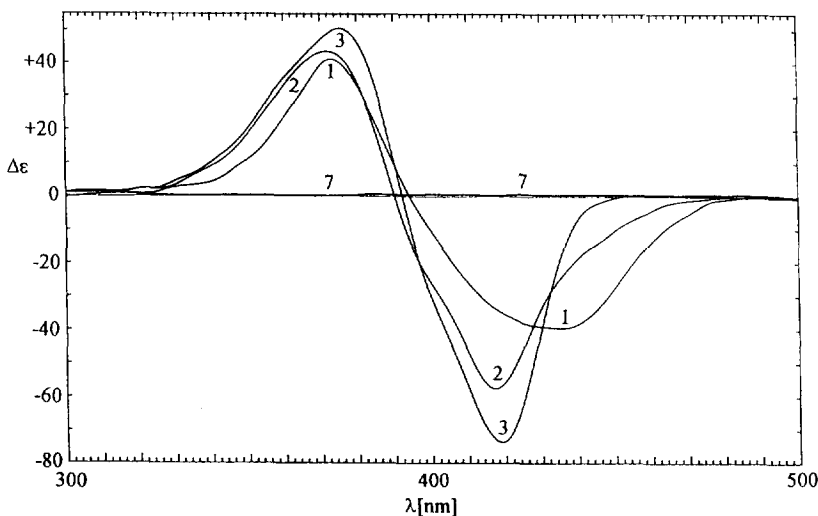


FIGURE 2. Circular dichroism spectra of 1.5×10^{-5} M solutions of bilirubin analogs **1-3** and dipyrinone **7** in chloroform at 22°C. The number beside each curve corresponds to pigment **1**, **2**, **3** or **7**.

coupling). The component dipyrinone chromophores of the bichromophoric rubins have strongly-allowed long-wavelength electronic transitions (Table 1) and interact through resonance splitting, *i.e.*, by electrostatic interaction of the local transition moment dipoles, which are oriented along the long axis of each dipyrinone (Fig. 1). This intramolecular exciton splitting interaction produces two long wavelength transitions in the UV-vis spectrum and two corresponding bands in the CD spectrum. One band is higher in energy, and one is lower in energy, with the splitting being dependent on the strength and relative orientation of the dipyrinone electric dipole transition moments. According to exciton chirality theory,¹⁸ a long wavelength negative, short wavelength positive CD couplet indicates a negative exciton chirality and a negative helical disposition of the relevant dipyrinone long wavelength transition moments. Usually this corresponds to the *M*-helical enantiomeric type of Fig. 1,¹¹ but, as has been

shown previously, opening of the interplanar angle of either enantiomer without inverting molecular chirality can cause the transition moments to invert helicity and thus invert the Cotton effect signs of the couplet.^{5a}

TABLE 1. Circular Dichroism and UV-Visible Spectral Data for Dipyrinones 7-9.

Dipyrinone	Solvent	Circular Dichroism			UV-Visible	
		$\Delta\epsilon^{\max}(\lambda_1)$	λ_2 at $\Delta\epsilon=0$	$\Delta\epsilon^{\max}(\lambda_3)$	ϵ^{\max}	$\lambda(\text{nm})$
7	CCl ₄	<0.1 (400)	—	—	43,400	(413)
8		+1.53 (397)	425	-0.80 (441)	44,100	(410)
9		+0.74 (400)	415	-0.65 (439)	42,000	(408)
7	Benzene	<0.1 (400)	—	—	41,200	(411)
8		+0.85 (392)	423	-0.59 (441)	41,000	(409)
9		+1.47 (403)	425	-0.57 (440)	39,900	(408)
7	CHCl ₃	<0.1 (400)	—	—	32,900	(410)
8		+0.82 (399)	—	<0.1 (440)	34,000	(407)
9		-1.63 (407)	416	+2.89 (439)	33,200	(406)
7	(CH ₃) ₂ CO	<0.1 (400)	—	—	35,200	(405)
8		+0.66 (394)	—	<0.1 (440)	35,300	(403)
9		<0.1 (400)	—	<0.1 (440)	35,000	(403)
7	CH ₃ OH	<0.1 (400)	—	—	37,800	(416)
8		<+0.1 (390)	—	—	38,800	(413)
9		<+0.1 (400)	—	—	38,600	(414)
7	CH ₃ CN	<0.1 (400)	—	—	34,100	(403)
8		<+0.1 (390)	—	—	34,200	(401)
9		<+0.1 (400)	—	—	34,000	(400)

Circular Dichroism and Conformation. The effectiveness of the 8¹S,12¹S methyls of 1-3 in displacing the *M* ⇌ *P* conformational equilibrium may be seen in their CD spectra (Fig. 2). Unlike simple dipyrinones, the CD spectra of 1-3 are indicative of strong exciton coupling,^{5,8,11,18} and the signed order of the Cotton effects implies a negative (*M*-helical) orientation of the component dipyrinone long wavelength electric transition dipole moments. This means the rubins must adopt preferentially a chiral conformation without the benefit of conformational stabilization provided by intramolecular hydrogen bonds (Fig. 1).^{5,11} When carboxylic acid groups are present and properly located to stabilize the ridge-tile conformations, more intense exciton CD Cotton effects are seen — as in the optically active, intramolecularly hydrogen-bonded (βS,β'S)-dimethylmesobilirubin-XIIIα (22) (Fig. 3).^{5a,8a} It is clear from Fig. 3 that (i) diacid 22 and 1-3 share the same signed-sequence for their bisignate CD Cotton effects, and (ii) while the 1 and 2 have Cotton effects with similar magnitudes, they are much less intense than either 22 or 3, which exhibit Cotton effects of comparable intensity. The intensity differences appear to be linked to the fact that the diacid 22 can stabilize the *M*-helicity ridge-tile enantiomer using a full complement of six intramolecular hydrogen bonds (Fig. 1); whereas, 1 and 2 cannot, and 3 can participate in minimal intramolecular hydrogen bonding using the two acetamide NHs. Although amide carbonyls are thought to be better hydrogen bond acceptors than ester carbonyls, the amide carbonyl of 3 and ester 2 are probably too far removed to be involved effectively in hydrogen bonding.

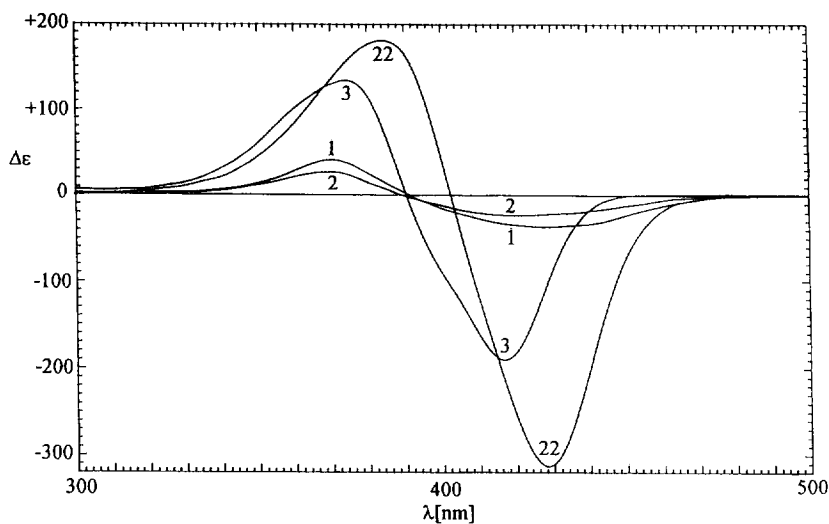


FIGURE 3. Circular dichroism spectra of 1.5×10^{-5} M solutions of bilirubin analogs (**1-3**) and (β S, β' S)-dimethylmesobilirubin-XIIIa (**22**) in acetonitrile at 22°C. The number beside each curve corresponds to pigment **1**, **2**, **3** or **22**.

The sensitivity of the CD data to changes in solvent may be noted in Table 2: **1** and **2** are only moderately sensitive to vastly different solvent polarity (dipoles) and hydrogen-bonding ability. In contrast, although the $\Delta\epsilon$ values for **3** tend to be larger than those of **1** and **2**, they range from a high of $\Delta\epsilon_{436}^{\max} - 322$ in cyclohexane to $\Delta\epsilon_{419}^{\max} - 74$ in CHCl_3 , to a low of $\Delta\epsilon_{426}^{\max} - 22$ in $(\text{CH}_3)_2\text{SO}$. The lower $\Delta\epsilon$ values of **3** tend to appear in solvents that participate in hydrogen bonding, and the highest values are not restricted to nonpolar solvents. On the other hand, with a full complement of six intramolecular hydrogen bonds (Fig. 1), as in diacid **22**, the $\Delta\epsilon$ values resist solvent perturbation over the entire scope of solvents and remain within 10-20% of the value seen in benzene ($\Delta\epsilon_{434}^{\max} - 362$) — except in the special case of $(\text{CH}_3)_2\text{SO}$, where $\Delta\epsilon_{422}^{\max} - 24$.^{8a} Nevertheless, the data of Table 2 suggest that even the most minimal intramolecular hydrogen bonding (as in **3**) can stabilize a particular ridge-tile shape in the absence of strong solvent perturbation and that hydrogen bonding is not essential to the diastereoselectivity of the *M*-helical conformer over the *P*. Diastereoselectivity apparently derives exclusively from the pigment's simply adopting a shape that minimizes intramolecular nonbonded steric interactions. For the (8^1 S, 12^1 S) configuration of **1-3** and **22** this means a preference for the *M*-helical conformer of Fig. 1.^{5,8a,11}

Consistent with these conclusions, exciton analysis⁵ of the UV-visible spectra (Table 2) suggests that the folded enantiomeric conformers probably favor a ridge-tile helical shape rather than a more extended shape. Unlike bilirubin and its analog **22**, which have UV-vis spectra with a more dominant long wavelength exciton component, the spectra of **1-3** indicate that the shorter wavelength exciton component is more intense than the long wavelength component in most of the solvents studied, especially for **1** and **2**, but less so for **3**. These data suggest the prevalence of conformations for **1-3** with an interplanar angle smaller than the 100° found in **22** and bilirubin, e.g., a more acute ridge-tile tending toward a helical conformation, or to a distorted ridge-tile.¹⁹ But it is difficult to predict with certainty the size of the interplanar angle from the UV-vis or CD data.

Stereochemistry from NMR: Nuclear Overhauser Effects. Additional experimental evidence for a folded conformation of *M*-helicity in **1-3** comes from NMR studies in CDCl_3 . A *syn-Z* configuration of the dipyrinones is established by: (i) strong $^1\text{H}\{^1\text{H}\}$ -NOEs between the pyrrole and lactam NHs and (ii) NOEs between the vinyl hydrogens at C(5)/C(15) and the methyls at C(7)/C(13) and the C(3)/C(17) ethyl CH_2 groups. NOEs between the $8^1/12^1$ CHs and the C(10) CH_2 , and between the CH_3 s at $8^1/12^1$ and the C(7)/C(13) CH_3 s indicates a preference

TABLE 2. Comparison of CD and UV Spectral Data from 1.5×10^{-5} M Solutions of Rubins (1-3).

Fig-ment	Solvent	ϵ^a	Circular Dichroism			UV-Visible			
			$\Delta\epsilon^{\max}(\lambda_1)$	λ_2 at $\Delta\epsilon=0$	$\Delta\epsilon^{\max}(\lambda_3)$	ϵ^{\max}	$\lambda(\text{nm})$	ϵ^{\max}	$\lambda(\text{nm})$
1	Cyclohexane	2.0	+50.4 (372)	393	-46.3 (440)	70,300	376	12,600	434 ^{sh}
2			+37.3 (369)	391	-34.0 (423)	76,300	375	15,200	426 ^{sh}
3			+157.5 (397)	410	-322.0 (436)	60,700	400	35,800	433
1	1,4-Dioxane	2.2	+35.9 (373)	394	-35.0 (439)	59,700	378		
2			+15.2 (369)	402	-18.2 (433)	63,800	377		
3			+69.5 (377)	391	-116.8 (418)	51,100	391	49,700	411
1	Benzene	2.3	+42.8 (374)	394	-45.1 (440)	67,700	380	14,000	432 ^{sh}
2			+39.1 (371)	391	-41.3 (421)	72,700	377	15,300	430 ^{sh}
3			+91.4 (378)	392	-154.1 (419)	49,500	389	38,400	415 ^{sh}
1	CHCl ₃	4.7	+42.2 (373)	394	-40.1 (433)	64,700	379	15,300	430 ^{sh}
2			+39.3 (373)	389	-58.3 (416)	62,300	378		
3			+50.4 (376)	392	-73.7 (419)	48,600	391	46,100	408 ^{sh}
1	CH ₃ CO ₂ C ₂ H ₅	6.0	+46.2 (370)	392	-40.3 (432)	69,300	374	15,300	424 ^{sh}
2			+24.7 (369)	391	-21.2 (418)	76,400	374		
3			+103.1 (375)	390	-170.5 (417)	51,900	387	46,600	410 ^{sh}
1	(CH ₃) ₂ CO	20.7	+44.8 (370)	392	-40.5 (425)	64,000	376	20,600	422 ^{sh}
2			+23.2 (373)	391	-21.9 (419)	69,700	374		
3			+130.5 (376)	392	-198.2 (419)	53,100	389	48,600	411 ^{sh}
1	CH ₃ CH ₂ OH	24.3	+17.7 (388)	403	-21.1 (434)	47,300	394	46,000	425
2			+26.0 (379)	397	-32.0 (425)	51,900	393	52,500	420
3			+45.7 (382)	400	-52.8 (426)	50,600	396	50,600	419
1	CH ₃ OH	32.6	+17.3 (382)	403	-20.0 (430)	46,700	395	47,300	425
2			+26.2 (379)	397	-32.8 (424)	52,200	393	51,800	417
3			+53.7 (380)	399	-65.4 (425)	51,000	394	50,100	417
1	CH ₃ CN	36.2	+41.7 (370)	392	-37.7 (429)	66,900	375	13,300	430 ^{sh}
2			+27.0 (370)	389	-23.9 (421)	73,700	373		
3			+133.8 (375)	391	-190.9 (417)	52,400	388	45,900	412 ^{sh}
1	(CH ₃) ₂ NCHO	36.7	+17.7 (376)	395	-24.2 (425)	46,400	392	50,300	423
2			+24.4 (378)	394	-26.5 (421)	53,400	389	53,700	417
3			+45.6 (379)	396	-61.6 (422)	50,600	391	49,700	417
1	(CH ₃) ₂ SO	46.5	+19.7 (386)	398	-29.7 (428)	43,800	398 ^{sh}	55,400	430
2			+26.5 (382)	398	-28.7 (423)	52,000	398 ^{sh}	58,600	425
3			+31.0 (384)	403	-22.2 (426)	47,300	397 ^{sh}	54,800	428
1	CH ₃ NHCHO	181.2	+16.6 (387)	403	-20.8 (432)	49,500	393	42,700	425
2			+20.2 (383)	399	-24.2 (427)	54,400	390	46,900	418
3			+37.4 (379)	399	-44.5 (425)	48,700	394	47,100	420

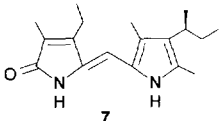
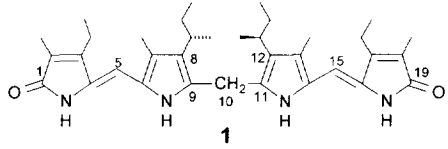
^a Dielectric constants from Gordon, A.J.; Ford, R.A. *The Chemist's Companion*, Wiley, NY (1972), pp 4-8.

for the *M*-helicity conformation in the 8¹S,12¹S enantiomer. Here the 8¹,12¹-methines are brought into close proximity to the C(10) CH₂ hydrogens, and the 8¹,12¹ methyls lie near the methyls at C(7) and C(13). (In the *P*-helicity conformation the opposite occurs, with the 8¹,12¹ methyls lying close to the C(10) CH₂, and the 8¹,12¹ methines lying close to the C(7)/C(13)-methyls.) These data are quite similar to those seen in **22**: the signals for

the C(7)/C(13) methyls and the β,β' -methyls are also related by a strong NOE, as are the β -CHs and the C(10) CH₂. In **22** other NOEs are found between the lactam and pyrrole NHs, between C(5)/C(15) hydrogens and the C(3)/C(17)-ethyl and C(7), C(13)-methyl groups, confirming that the dipyrinones adopt a *syn-Z* conformation. Direct evidence for an intramolecularly hydrogen-bonded conformation of **22** comes from irradiation of the carboxylic acid hydrogen (COOH) and observing a 4.5% NOE on the lactam NHs. These findings are consistent with the predictions of the exciton chirality rule and the data of Table 2.

Interestingly, weak NOEs were also detected between the methyls at C(2)/C(18) and (i) the C(10) CH₂ and (ii) the pyrrole NHs of **1-3**. Such NOEs may be taken to indicate the presence of dimers formed by *intermolecular* hydrogen bonding between dipyrinone units. Similar NOEs were reported previously for dipyrinones such as kryptopyrromethenone and methyl xanthobilirubinate, where dipyrinone to dipyrinone dimeric association through intermolecular hydrogen bonding prevailed in nonpolar solvents such as chloroform, but not in more polar solvents, such as dimethylsulfoxide.²⁰ This is consistent with the dimeric structure suggested for bilirubin dimethyl ester based on conclusions from NOE and vapor pressure osmometry studies.¹⁹ However, unlike dipyrinones, little if any effect of dilution is seen on the NH chemical shifts (Table 3). Thus, one may assume a dimer for **1** with $K_{\text{assoc}} \gg 10^4$, inasmuch as K_{assoc} for dipyrinones is $\sim 25,000$ M in CDCl₃ at 22 °C.^{19,20} In CDCl₃ - 10% (CD₃)₂SO solvent, the intermolecular NOEs vanish, while the same intramolecular NOEs as above are maintained. The small amount of added (CD₃)₂SO is sufficient to disrupt the dimeric association but is known to be insufficient to disengage intramolecular hydrogen bonding in bilirubin.²¹ It is important to note that despite the potential for dimer formation in nonpolar solvents, the CD spectra of **1-3** maintain the same Cotton effect signs over a wide range of solvent polarity, with the magnitudes of **1** and **2** being nearly the same over the range (Table 2). The origin of the exciton appears thus to be largely *intra* rather than *intermolecular*.

TABLE 3. Concentration Dependence of Pyrrole and Lactam NH Chemical Shifts in CDCl₃ Solutions.

Concentration [M]	 7		 1	
	Lactam NH	Pyrrole NH	Lactam NH	Pyrrole NH
2×10^{-2}	11.30	10.28	10.77	10.17
5×10^{-3}	11.16	10.18	10.77	10.17
5×10^{-4}	10.67	9.88	10.77	10.17
5×10^{-5}	10.33	9.73	10.77	10.17

Conformational Analysis from Molecular Mechanics Calculations. A conformational energy map correlating a multiplicity of bilirubin conformations may be created from the results of molecular dynamics calculations.⁵ In this study, we determined the range of conformations created by rotating a rubin's two dipyrinones independently about the C(9)-C(10) and C(10)-C(11) bonds in steps of 10°. The conformations are defined by the

corresponding torsion angles, $\phi_1 = \text{N}(22)\text{-C}(9)\text{-C}(10)\text{-C}(11)$ and $\phi_2 = \text{C}(9)\text{-C}(10)\text{-C}(11)\text{-N}(23)$, where $\phi_1 = \phi_2 = 0^\circ$ corresponds to a planar porphyrin-like shape, which is very high energy, and $\phi_1 = \phi_2 \sim 180^\circ$ corresponds to the linear shape (Synthetic Scheme), which is also very high energy.⁵ For **1**, the conformational energy map (Fig. 4) shows that these very high energy conformations lie atop full peaks surrounded by valleys or canyons containing several potential energy wells that correspond to global and local minima. The global minimum conformation found at $\phi_1 = \phi_2 \sim -50^\circ$ has the typical ridge-tile shape (**M**, Figs. 5 and 1), albeit with twisted rather than planar dipyrinones. Two local minima, essentially isoenergetic with the global minimum, lie nearby at $\phi_1 \sim -110^\circ$, $\phi_2 \sim +50^\circ$ and $(\phi_1 \sim -60^\circ, \phi_2 \sim +140^\circ)$ — along a canyon or path connecting the **M**-helicity ridge-tile with the **P**-helicity ridge-tile shape local minimum at $\phi_1 = \phi_2 \sim +70^\circ$ (Fig. 5). The energy barriers separating these local minima are low. Two other local minima, $(\phi_1 = \phi_2 \sim -130^\circ)$ and $(\phi_1 = \phi_2 \sim +120^\circ)$ lie nearby the **M** and **P**-helicity ridge-tile minima, respectively, and correspond to nearby enantiomeric, extended or stretched conformations (Fig. 5). Subject to modification due to solvation effects, the data suggest that **1** adopts mainly the $(\phi_1 = \phi_2 \sim -50^\circ)$, $(\phi_1 \sim -110^\circ, \phi_2 \sim +50^\circ)$ and $(\phi_1 \sim -60^\circ, \phi_2 \sim +140^\circ)$ conformations.

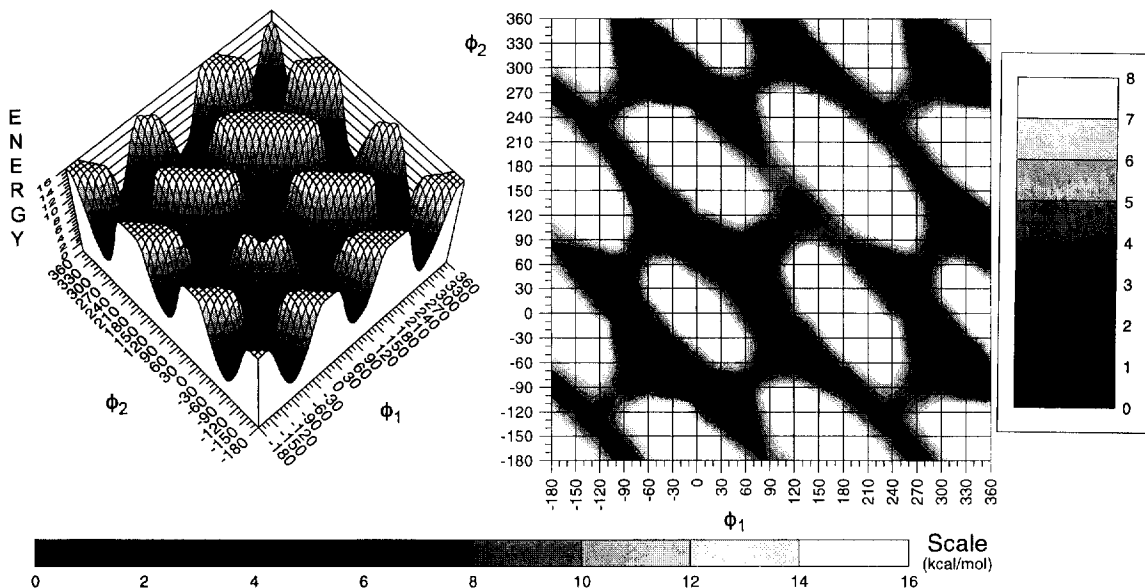


FIGURE 4. Conformational energy surface (left) and its energy scale (below), and contour map (right) and its energy scale for mesobilirubin analog **1** conformers generated by rotating its two dipyrinones independently about the $\text{C}_9\text{-C}_{10}$ and $\text{C}_{10}\text{-C}_{11}$ carbon-carbon single bonds (ϕ_1 and ϕ_2 , respectively) in steps of 10° . The global minimum (set to 0.0 kcal/mole) is found near $\phi_1 = \phi_2 \sim -50^\circ$, corresponding to the **M**-helicity enantiomer. Local minima are found near $\phi_1 \sim -110^\circ$, $\phi_2 \sim +50^\circ$; $\phi_1 \sim -60^\circ$, $\phi_2 \sim +140^\circ$; $\phi_1 = \phi_2 \sim +70^\circ$ (**P**-helicity ridge-tile) $\phi_1 = \phi_2 \sim +120^\circ$, and $\phi_1 = \phi_2 \sim -130^\circ$, lying 0.1, 0.3, 1.1, 1.1 and 2.2 kcal/mole above the global minimum. Data are from molecular dynamics simulations using SYBYL® (Tripos Assoc.) on an Evans & Sutherland ESV-10 workstation according to ref. 5. The energy displays were created using Wingz™ (Informix).

Significantly, the global minimum conformation of **1** has nearly the same shape as the global minimum conformation of bilirubin (Fig. 1), or more specifically that of analog **22**: the **M**-helicity ridge-tile. The major geometric difference lies in the slightly twisted dipyrinones of **1**; whereas, in the intramolecularly hydrogen-bonded

analog (**22**) the dipyrinones are nearly planar. In both **1** and **22** the global minimum conformation is one where nonbonded steric repulsions are minimized, but in **22** this conformation is further stabilized by six intramolecular hydrogen bonds, which is significant (~ 20 kcal/mole). Thus, in the conformational energy map of **22**,^{8a} the energy wells corresponding to the *M*-helicity global and *P*-helicity local minima are much deeper, and the interconversion barriers are higher (~ 20 kcal/mole) between the *M*-helicity global minimum and the *P*-helicity local minimum (which lies ~ 4.3 kcal/mole above the global minimum).⁵ Thus, **22** exhibits very intense CD (Fig. 3). In **1**, on the other hand, interconversions barriers between global and local minima are much lower, and the energy differences among the minima are also smaller. This means that the CD spectrum (Fig. 3) seen for **1** is actually the population weighted sum of the CDs of each contributing conformation — according to molecular dynamics computations, mainly those corresponding to $(\phi_1 = \phi_2 \sim -50^\circ)$, $(\phi_1 \sim -110^\circ, \phi_2 \sim +50^\circ)$ and $(\phi_1 \sim -60^\circ, \phi_2 \sim +140^\circ)$. Since **1** exhibits a CD of $\sim 15\%$ of the intensity of **22**, it would appear that while the contribution of the *M*-chirality conformation at $(\phi_1 = \phi_2 \sim -50^\circ)$ dominates the CD, the net contributions of the other contributing conformations are nearly self-cancelling, as would be expected from the structures and relative energies of Fig. 5.

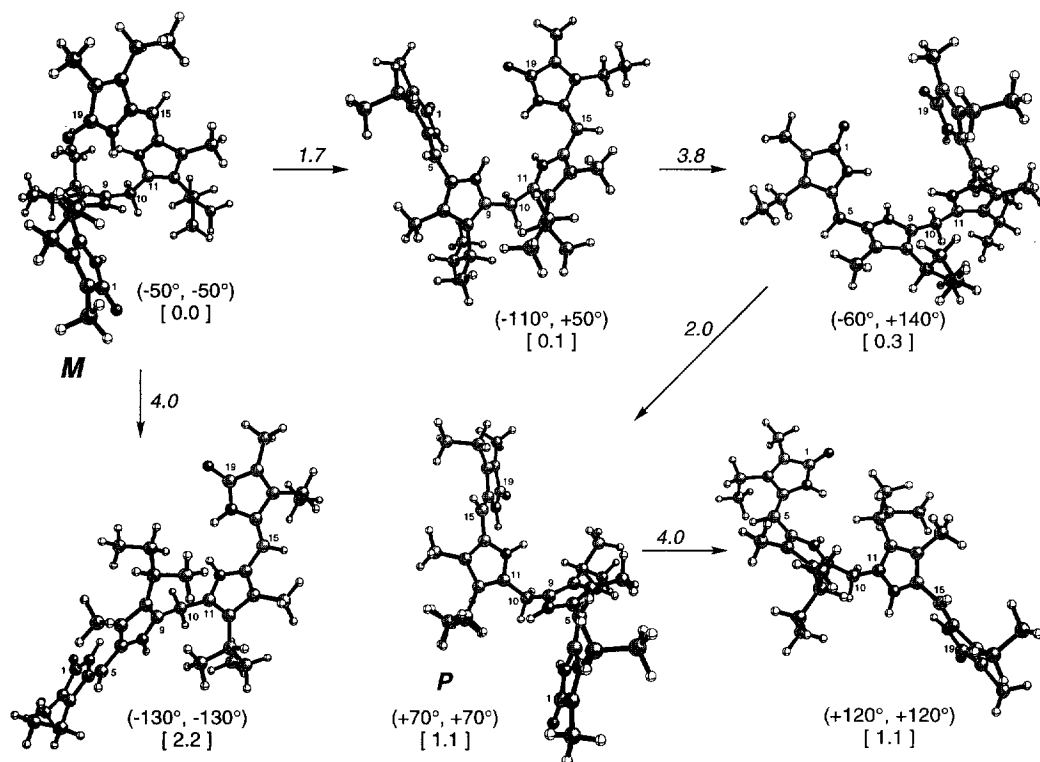


FIGURE 5. Ball and stick conformational representations relating the ridge-tile shaped *M*-helicity global minimum to local minima. Conformational representatives were created using Müller and Falk's "Ball and Stick." Structures are identified by torsion angles (ϕ_1, ϕ_2) and their relative energies in brackets, [kcal/mole]. The energy barriers in kcal/mole are given next to the arrows.

Although the foregoing molecular dynamics conformational analysis is for *unsolvated* **1** and **22**, it may be used to gain insight into the probable shape of the pigment when it is monomeric in solution, as in the higher

dielectric solvents of Table 2. In nonpolar solvents a dimer is apparently dominant; so we modelled dimers of **1** in order to extract information on the stereochemistry of each pigment unit. These results are summarized in the dimeric structures of Figure 6. In the energy-minimum dimer, the two monomer units have essentially identical conformations, with $\phi_1 \sim -95^\circ$, $\phi_2 \sim +13^\circ$ and $\phi_1 \sim -95^\circ$, $\phi_2 \sim +100^\circ$ corresponding to an *M*-helical rubin. These conformations are predicted^{5a} to exhibit strong negative exciton coupling CD spectra. For comparison, the dimer formed of *P*-helicity monomer units of **1** (Figure 6) lies 0.7 kcal/mole higher energy, and the two monomer units have essentially identical conformations, with $\phi_1 \sim +100^\circ$, $\phi_2 \sim -21^\circ$ and $\phi_1 \sim +100^\circ$, $\phi_2 \sim -27^\circ$. These conformations are predicted to exhibit strong positive exciton coupling Cotton effects. And the dimer formed from *M* and *P*-helical components cannot adopt more than two hydrogen bonds and is higher energy. Since the *M*-helical dimer is slightly favored over the *P*, the observed moderate, negative exciton Cotton effects observed in nonpolar solvents (Table 2) are supported by this molecular mechanics analysis of conformation.

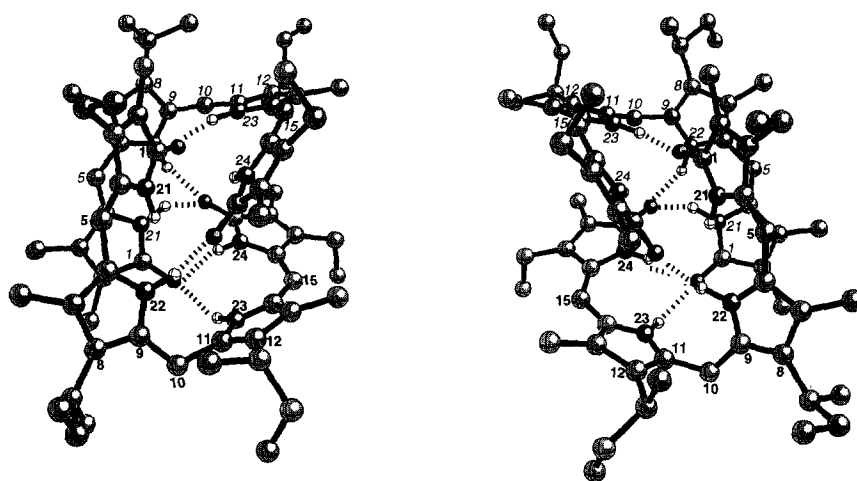


FIGURE 6. Ball and stick representations for low-energy dimers of **1**. (Left) Minimum energy dimer of **1** held by intermolecular hydrogen bonds between the component dipyrinones. In each component of the dimer, $\phi_1 \sim -95^\circ$, $\phi_2 \sim +13^\circ$, corresponding to an *M*-helicity. (Right) Higher energy dimer of **1** where each component adopts a *P*-helicity with $\phi_1 \sim +100^\circ$, $\phi_2 \sim -27^\circ$. Hydrogens are removed from carbons for clarity of representation. Hydrogen bonds are shown by hatchmarks. In each dimer, bold numbering corresponds to one monomer unit; italics numbering corresponds to the second monomer unit.

CONCLUDING COMMENTS

Intramolecular hydrogen bonding, which is characteristic of natural bilirubin, is known to be a dominant force in determining the pigment's conformation (Fig. 1). The current study shows that when the propionic acids at C(8) and C(12) are replaced by alkyl or ether groups having stereogenic centers at 8¹ and 12¹, **1** and **2** are forced by nonbonded steric interactions to adopt an *M*-helicity conformation. When residual intramolecular hydrogen bonding is possible, as in amide **3**, the *M*-helicity shaped ridge-tile conformer is dominant. Molecular dynamics computations support the interesting and surprising result derived from spectroscopy: the *M*-helicity conformation is clearly favored, even in the absence of intramolecular hydrogen bonding.

EXPERIMENTAL

General. All circular dichroism spectra were recorded on a JASCO J-600 instrument, and all UV-vis spectra were recorded on a Perkin Elmer Lambda 12 or Cary 219 spectrophotometer. NMR spectra were obtained on a GN-300 or Varian Unity Plus spectrometers operating at 300 MHz and 500 MHz, respectively. CDCl_3 solvent was used throughout and chemical shifts were reported in δ ppm referenced to residual CHCl_3 ^1H signal at 7.26 ppm and ^{13}C -signal at 77.00 ppm. J-modulated spin-echo experiments (*Attached Proton Test*) were used to obtain the ^{13}C -NMR assignments. Optical rotations were measured on a Perkin Elmer model 141 polarimeter. HPLC analyses were carried out on a Perkin Elmer Series 410 high-pressure liquid chromatograph with a Perkin Elmer LC-95 UV-vis spectrophotometric detector (set at 420 nm) equipped with a Beckman Altex ultrasphere IP 5 μm C-18 ODS column (25×0.46 cm) kept at 34°C . The flow rate was 1.0 mL min^{-1} and the mobile phase was 0.1 M di-*n*-octylamine acetate buffer in 5% aqueous methanol (pH 7.7 at 25°C). Radial chromatography was carried out on Merck Silica gel PF₂₅₄ with CaSO_4 preparative layer grade, using a Chromatotron (Harrison Research, Inc., Palo Alto, CA) with 1, 2 or 4 mm thick rotors. Melting points were determined on a Mel-Temp capillary apparatus and are uncorrected. Combustion analyses were carried out by Desert Analytics, Tucson, AZ.

The spectral data were obtained in spectral grade solvents (Aldrich or Fisher). HPLC grade solvents were dried and purified following standard procedures.²² All commercial reagents were from Aldrich or ACROS.

The starting compounds: **optically pure (+)-3(S)-(2,4-dimethyl-5-ethoxycarbonyl-1H-pyrrol-3-yl)butanoic acid (14)**,^{8a} **(+)-methyl 3(S)-(4-ethyl-3,8,10-trimethyl-2-oxo-1,11-dihydrodipyrin-9-yl)butanoate (15)**,^{8a} **(+)-3(S)-(2,4-dimethyl-5-ethoxycarbonyl-1H-pyrrol-3-yl)butan-1-ol (13)** and its *p*-toluenesulfonate **(12)**,¹⁵ and **(-)-3(S)-(4-ethyl-3,8,10-trimethyl-2-oxo-1,11-dihydrodipyrin-9-yl)butanoic acid (16)**¹⁵ were synthesized as described previously.

(+)-Ethyl 3,5-dimethyl-4-[1(S)-methylpropyl]-1H-pyrrole-2-carboxylate (10). A mixture of 3.93 g (10 mmol) of tosylate **12**, 7.50 g (50 mmol) of NaI, 6.54 g (100 mg-A) Zn, 100 mL of 1,2-dimethoxyethane, and 4 mL of H_2O were combined and heated under reflux for 3h. After cooling, the mixture was filtered and the filtered solid was washed with 3×30 mL of CH_2Cl_2 . The combined filtrates were washed with 5% HCl (2×35 mL), H_2O (3×50 mL) then dried over anhydrous MgSO_4 and filtered. The solvent was removed under vacuum to afford the crude product (2.22 g, quantitative yield), which was used in the next step without further purification. An analytical sample was obtained after recrystallization from ethyl acetate-hexane. It had mp $95\text{--}96^\circ\text{C}$; $[\alpha]_{\text{D}}^{20} + 24.0^\circ$ (*c* 1.3, $\text{C}_2\text{H}_5\text{OH}$); $^1\text{H-NMR}$: δ 0.81 (3H, t, $J=7.4$ Hz), 1.22 (3H, d, $J=7.2$ Hz), 1.34 (3H, t, $J=7.1$ Hz), 1.55-1.65 (2H, m), 2.22 (3H, s), 2.31 (3H, s), 2.57-2.64 (1H, m), 4.29 (2H, q, $J=7.1$ Hz), 8.58 (1H, br.s) ppm and $^{13}\text{C-NMR}$: δ 11.06, 12.68, 12.71, 14.58, 20.41, 29.42, 32.45, 59.49, 116.56, 125.81, 126.98, 129.00, 161.76 ppm.

Anal. Calcd. for $\text{C}_{13}\text{H}_{21}\text{NO}_2$ (223.3): C, 69.92; H, 9.48; N, 6.27.

Found: C, 69.89; H, 9.53; N, 6.35.

(+)-3(S)-(4-Ethyl-3,8,10-trimethyl-2-oxo-1,11-dihydrodipyrin-9-yl)butan-1-ol (17). To an N_2 -blanketed, cooled (-20°C) solution of 1.58 g (5 mmol) of acid **16** and 0.84 mL (6 mmol) of dry triethylamine in 40 mL of dry THF was added 0.60 mL (6 mmol) of ethyl chloroformate. The mixture was stirred for 15 min and the resulting precipitate was filtered and washed with 2×5 mL portions of dry THF under N_2 protection. To the filtrate was added sodium borohydride (230 mg, 6 mmol) at -20°C , followed by 4 mL of dry methanol. The mixture was

stirred for 2h at -20°C , and the reaction was quenched with 10 mL of H_2O . The mixture was diluted with 250 mL of CHCl_3 , washed with H_2O (2×200 mL), dried (anhydrous Na_2SO_4) and filtered. The solvent was removed under vacuum, and the resulting product was triturated with 5 mL of CH_3OH and 20 mL of dry ether to afford 1.38 g, 91% of pure alcohol **17**, which was used in the next step. An analytically pure sample was obtained after radial chromatography (4% $\text{CH}_3\text{OH}/\text{CH}_2\text{Cl}_2$ eluent) and recrystallization from $\text{CH}_3\text{OH}/\text{Et}_2\text{O}$. It had mp $226\text{-}227^{\circ}\text{C}$ (decomp.), $[\alpha]_{\text{D}}^{20} +54.3^{\circ}$ (c 0.5, CHCl_3); $^1\text{H-NMR}$: δ 1.17 (3H, t, $J=7.6$ Hz), 1.24 (1H, br.t), 1.28 (3H, d, $J=7.2$ Hz), 1.85-1.91 (2H, m), 1.94 (3H, s), 2.18 (3H, s), 2.46 (3H, s), 2.55 (2H, q, $J=7.6$ Hz), 2.87-3.00 (1H, m), 3.55-3.63 (2H, m), 6.14 (1H, s), 10.32 (1H, br.s), 11.30 (1H, br.s) ppm; and $^{13}\text{C-NMR}$: δ 8.55, 10.39, 12.63, 15.05, 17.96, 21.04, 27.58, 39.18, 62.11, 100.93, 122.35, 122.45, 123.91, 124.22, 127.15, 131.03, 148.37, 174.11 ppm.

Anal. Calcd. for $\text{C}_{18}\text{H}_{26}\text{N}_2\text{O}_2$ (302.4): C, 71.49; H, 8.67; N, 9.26.

Found: C, 70.95; H, 8.63; N, 8.92.

(-)-3(S)-(4-Ethyl-3,8,10-trimethyl-2-oxo-1,11-dihydropyrrin-9-yl)butan-1-ol *p*-toluenesulfonate (18). A mixture of 1.31 g (4.3 mmol) of alcohol **17**, 22 mL of dry CH_2Cl_2 , and 1.2 mL (8.6 mmol) of Et_3N was cooled with ice bath and it was added 1.65 g (8.6 mmol) of *p*-toluenesulfonyl chloride over 20 min. After stirring 14h at room temperature, the reaction mixture was diluted with 300 mL of CHCl_3 and washed with 1% of HCl (100 mL) then water (3×200 mL). After drying over anhydrous Na_2SO_4 and filtering, the solvent was evaporated under vacuum. The crude product was purified by radial chromatography (eluent: 1.5-3% CH_3OH in CH_2Cl_2) and recrystallized from CHCl_3 - CH_3OH to afford 1.55 g (79%) of tosylate **18**. It had mp $160\text{-}162^{\circ}\text{C}$; $[\alpha]_{\text{D}}^{20} -40.3^{\circ}$ (c 0.4, CHCl_3); $^1\text{H-NMR}$: δ 1.18 (3H, t, $J=7.6$ Hz), 1.22 (3H, d, $J=7.0$ Hz), 1.95 (3H, s), 1.92-1.99 (2H, m), 2.08 (3H, s), 2.36 (3H, s), 2.39 (3H, s), 2.55 (2H, q, $J=7.6$ Hz), 2.88 (1H, dq, $J=7.0$; 7.0 Hz), 3.82-3.90 (1H, m), 3.96-4.03 (1H, m), 6.10 (1H, s), 7.29 (2H, d, $J=8.2$ Hz), 7.72 (2H, d, $J=8.2$ Hz), 10.28 (1H, br.s), 11.35 (1H, br.s) ppm; and $^{13}\text{C-NMR}$: δ 8.56, 10.30, 12.48, 15.06, 17.96, 20.68, 21.55, 26.86, 35.28, 69.59, 100.90, 122.38, 122.43, 122.56, 124.16, 127.12, 127.79, 129.71, 131.14, 133.14, 144.54, 148.43, 174.13 ppm.

Anal. Calcd. for $\text{C}_{25}\text{H}_{32}\text{N}_2\text{O}_4\text{S}$ (456.6): C, 65.76; H, 7.06; N, 6.14.

Found: C, 65.49; H, 7.09; N, 6.06.

(+)-3(S)-(4-Ethyl-3,8,10-trimethyl-2-oxo-1,11-dihydropyrrin-9-yl)-1-iodobutane (19). A mixture of 1.37 g (3 mmol) of tosylate **18**, 4.50 g (30 mmol) of NaI , and 90 mL of dry acetone was stirred and heated at reflux vigorously for 3h. The solvent was evaporated under vacuum, and the residue was partitioned between 300 mL of CHCl_3 and 200 mL of H_2O . The organic layer washed with H_2O (3×100 mL), dried over anhydrous Na_2SO_4 and filtered. The solvent was evaporated under vacuum, and the resulting crude product was recrystallized from CHCl_3 - CH_3OH to afford 1.16 g (94%) of iodide **19**. It had mp $178\text{-}180^{\circ}\text{C}$; $[\alpha]_{\text{D}}^{20} +87.6^{\circ}$ (c 0.5, CHCl_3); $^1\text{H-NMR}$: δ 1.17 (3H, t, $J=7.6$ Hz), 1.27 (3H, d, $J=7.1$ Hz), 1.95 (3H, s), 2.01-2.11 (1H, m), 2.13-2.24 (1H, m), 2.18 (3H, s), 2.48 (3H, s), 2.55 (2H, q, $J=7.6$ Hz), 2.85-2.95 (1H, m), 3.02 (1H, dt, $J=9.1$; 7.7 Hz), 3.17 (1H, dt, $J=9.1$; 7.0 Hz), 6.14 (1H, s), 10.32 (1H, br.s), 11.30 (1H, br.s); and $^{13}\text{C-NMR}$: δ 6.18, 8.57, 10.51, 12.79, 15.05, 17.96, 20.40, 31.43, 40.14, 100.88, 122.38, 122.49, 122.65, 124.25, 127.18, 131.29, 148.39, 174.14 ppm.

Anal. Calcd. for $\text{C}_{18}\text{H}_{25}\text{IN}_2\text{O}$ (412.3): C, 52.43; H, 6.11; N, 6.79.

Found: C, 52.37; H, 6.05; N, 6.63.

(+)-3(S)-(4-Ethyl-3,8,10-trimethyl-2-oxo-1,11-dihydrodipyrriin-9-yl)-1-azidobutane (20). A mixture of 1.03 g (2.5 mmol) of iodide **19**, 813 mg (12.5 mmol) of sodium azide, and 55 mL of dry dimethylformamide was stirred at 50 °C for 4h. After cooling, it was diluted with 200 mL of CHCl₃, washed with H₂O (4 × 200 mL) and dried over anhydrous Na₂SO₄. After filtration, the solvent was evaporated under vacuum. The resulting crude product was recrystallized from CHCl₃-CH₃OH to afford 745 mg (91%) of azide **20**. It had mp 179-181 °C; $[\alpha]_D^{20} +91.8^\circ$ (c 0.5, CHCl₃); ¹H-NMR: δ 1.18 (3H, t, J=7.6 Hz), 1.29 (3H, d, J=7.2 Hz), 1.82-1.90 (2H, m), 1.95 (3H, s), 2.16 (3H, s), 2.45 (3H, s), 2.55 (2H, q, J=7.6 Hz), 2.83-2.96 (1H, m), 3.12 (1H, dt, J=12.1; 7.5 Hz), 3.26 (1H, dt, J=12.1; 6.7 Hz), 6.14 (1H, s), 10.34 (1H, br.s), 11.33 (1H, br.s) ppm; and ¹³C-NMR: δ 8.54, 10.33, 12.54, 15.05, 17.92, 20.76, 27.88, 35.15, 50.13, 100.86, 122.32, 122.40, 122.89, 124.16, 127.09, 131.08, 148.35, 174.10 ppm.

Anal. Calcd. for C₁₈H₂₅N₅O (327.4): C, 66.03; H, 7.70; N, 21.39.

Found: C, 65.96; H, 7.69; N, 21.40.

3-(4-Ethyl-3,8,10-trimethyl-2-oxo-1,11-dihydrodipyrriin-9-yl)-1-butyl amine (21). A mixture of 164 mg (0.5 mmol) of racemic azide **20**, 197 mg (0.75 mmol) triphenyl phosphine, 4 mL of THF and 0.3 mL of H₂O was heated under reflux for 3h. The solvents were evaporated under vacuum. Recrystallization of the residual from benzene-diethyl ether afforded 52 mg (34%) of amine **21**. It had mp 212-214 °C; ¹H-NMR: δ 1.15 (2H, very br.s), 1.17 (3H, t, J=7.6 Hz), 1.26 (3H, d, J=7.1 Hz), 1.72-1.80 (2H, m), 1.94 (3H, s), 2.16 (3H, s), 2.45 (3H, s), 2.55 (2H, q, J=7.6 Hz), 2.64 (2H, br.t, J=7.4 Hz), 2.80-2.87 (1H, m), 6.14 (1H, s), 10.33 (1H, br.s), 11.34 (1H, br.s) ppm; and ¹³C-NMR: δ 8.55, 10.39, 12.69, 15.08, 17.94, 21.00, 28.37, 40.57, 41.06, 100.99, 122.17, 122.23, 124.30, 124.39, 126.93, 130.93, 148.29, 174.04 ppm. This amine was generated *in situ* and reacted to form **9**.

(+)-4-Ethyl-9-[1(S)-methylpropyl]-3,8,10-trimethyl-2-oxo-1,11-dihydrodipyrriinone (7). A mixture of 1.56 g (7 mmol) of ethyl ester **10**, 1.40 g (35 mmol) of NaOH, 15 mL of ethanol, and 5 mL of water was heated at reflux for 3h. The solvents were removed under vacuum. To the residue was added 35 mL of methanol, and the mixture was carefully acidified with conc. HNO₃ at 0 °C. 5-Bromomethylene-4-ethyl-3-methyl-2-oxo-1H-pyrrole¹⁶ (1.51 g, 7 mmol) was added, and the mixture was heated at reflux for 7h. It was chilled overnight at -20 °C. The resulting precipitate was filtered and washed with cold methanol. The crude product was dissolved in CH₂Cl₂, filtered, evaporated and recrystallized from chloroform-methanol to afford 1.42 g (71%) of bright yellow dipyrriinone **7**. It had mp 241-242 °C; $[\alpha]_D^{20} +53.3^\circ$ (c 0.6, CHCl₃); ¹H-NMR: δ 0.84 (3H, t, J=7.3 Hz), 1.17 (3H, t, J=7.6 Hz), 1.25 (3H, d, J=7.1 Hz), 1.57-1.66 (2H, m), 1.95 (3H, s), 2.16 (3H, s), 2.45 (3H, s), 2.55 (2H, q, J=7.6 Hz), 2.59-2.67 (1H, m), 6.15 (1H, s), 10.28 (1H, br.s), 11.30 (1H, br.s) ppm; and ¹³C-NMR: δ 8.53, 10.34, 12.73, 12.83, 15.05, 17.95, 20.55, 29.58, 32.69, 101.15, 122.03, 122.15, 124.66, 124.92, 126.79, 131.18, 148.25, 174.03 ppm.

Anal. Calcd. for C₁₈H₂₆N₂O (286.4): C, 75.48; H, 9.15; N, 9.78.

Found: C, 74.97; H, 9.16; N, 9.75.

(+)-4-Ethyl-9-[1(S)-methyl-3-acetoxypropyl]-3,8,10-trimethyl-2-oxo-1,11-dihydrodipyrriinone (8). A mixture of 1.36 g (4.5 mmol) of alcohol **17**, 10 mL of dry pyridine, and 4.25 mL (45 mmol) of acetic anhydride was stirred for 16h. It was diluted with 150 mL of CH₂Cl₂, washed carefully with 5% NaHCO₃ (2 × 100 mL), H₂O (2 × 100 mL) and dried over anhydrous Na₂SO₄. After filtering, the solvent was removed under vacuum. The resulting solid was recrystallized from CHCl₃/CH₃OH to afford 1.37 g (88%) of bright yellow dipyrriinone **8**. It had mp

146-148°C; $[\alpha]_D^{20} +82.2^\circ$ (*c* 0.7, CHCl₃); ¹H-NMR: δ 1.18 (3H, t, *J*=7.6 Hz), 1.29 (3H, d, *J*=7.1 Hz), 1.94 (3H, s), 1.90-1.99 (2H, m), 2.03 (3H, s), 2.15 (3H, s), 2.44 (3H, s), 2.55 (2H, q, *J*=7.6 Hz), 2.85-2.93 (1H, m), 3.86-3.98, 4.00-4.09 (2 × 1H, 2 × m), 6.13 (1H, s), 10.32 (1H, br.s), 11.31 (1H, br.s) ppm; and ¹³C-NMR: δ 8.55, 10.30, 12.57, 15.04, 17.95, 20.84, 21.01, 27.38, 35.11, 63.57, 100.94, 122.31, 122.38, 123.39, 124.21, 127.10, 130.98, 148.34, 171.10, 174.10 ppm.

Anal. Calcd. for C₂₀H₂₈N₂O₃ (344.4): C, 69.74; H, 8.19; N, 8.13.

Found: C, 69.82; H, 8.24; N, 7.78.

(+)-4-Ethyl-9-[1(*S*)-methyl-3-acetamidopropyl]-3,8,10-trimethyl-2-oxo-1,11-dihydrodipyrinone (9). A mixture of 655 mg (2 mmol) of azide **20**, 20 mL of THF, 788 mg (3 mmol) of triphenyl phosphine, and 1.2 mL of H₂O was heated at reflux for 3h; then the solvents were evaporated under vacuum. The residual water was co-evaporated with 3 × 20 mL of dry benzene. The residue was diluted with 20 mL of dry CH₂Cl₂ and to it was added 2 mL of acetic acid, 6 mg of DMAP, and 1.24 g (6 mmol) dicyclohexylcarbodiimide. The mixture was stirred for 45 min., concentrated under vacuum to 10 mL, and filtered to remove dicyclohexylurea. The filtrate was purified by radial chromatography (eluent: 3-4.5% CH₃OH in CH₂Cl₂) and the chromatographically pure product was crystallized from CH₂Cl₂-dry Et₂O to afford 640 mg (93%) of acetamide **9**. It had 196-198°C; $[\alpha]_D^{20} +44.5^\circ$ (*c* 0.3, CHCl₃); ¹H-NMR: δ 1.17 (3H, t, *J*=7.6 Hz), 1.27 (3H, d, *J*=7.1 Hz), 1.81-1.89 (2H, m), 1.88 (3H, s), 1.94 (3H, s), 2.16 (3H, s), 2.44 (3H, s), 2.55 (2H, q, *J*=7.6 Hz), 2.74-2.83 (1H, m), 3.02-3.11 (1H, m), 3.25-3.34 (1H, m), 5.34 (1H, br.t), 6.13 (1H, s), 10.32 (1H, br.s), 11.30 (1H, br.s) ppm; and ¹³C-NMR: δ 8.52, 10.35, 12.57, 15.03, 17.90, 20.99, 23.26, 28.99, 35.83, 38.97, 100.74, 122.36, 122.41, 123.66, 123.92, 127.16, 130.75, 148.35, 169.92, 174.06 ppm.

Anal. Calcd. for C₂₀H₂₉N₃O₂ (343.5): C, 69.94; H, 8.51; N, 12.23.

Found: C, 70.24; H, 8.55; N, 12.22.

Mesobiliverdin-XIIIα analogs 4-6. General procedure. A mixture of 1 mmol of dipyrinone **7-9**, 615 mg (2.5 mmol) of *p*-chloranil, 220 mL of CH₂Cl₂, and 11 mL of formic acid (97%) was heated at reflux for 24h. The volume of the mixture was reduced by distillation to one half, and reflux was continued for 6h. Then the mixture was chilled overnight at -20°C. The separated solid was filtered, and the cold filtrate was carefully neutralized with saturated aqueous NaHCO₃. The organic layer was washed consecutively with 2 × 100 mL of 1 M NaOH and 4 × 200 mL of H₂O, then dried over anhydrous Na₂SO₄. After removing the solvent under vacuum, the crude product was purified by radial chromatography eluting with 1.5-2% CH₃OH in CH₂Cl₂ for **4** or **5**, and 3-5% CH₃OH in CH₂Cl₂ for **6** to afford bright blue mesobiliverdin-XIIIα analogs (**4-6**).

3,17-Diethyl-8,12-bis-[1(*S*)-methylpropyl]-2,7,13,18-tetramethyl-(21*H*,24*H*)-bilin-1,19-dione (4). This verdin was synthesized from dipyrinone **7** in 88% yield. It had mp 267-269°C; ¹H-NMR: δ 0.88 (6H, t, *J*=7.3 Hz), 1.22 (6H, t, *J*=7.6 Hz), 1.35 (6H, d, *J*=7.1 Hz), 1.67-1.77 (4H, m), 1.82 (6H, s), 2.11 (6H, s), 2.53 (4H, q, *J*=7.6 Hz), 2.77-2.87 (2H, m), 5.99 (2H, s), 6.94 (1H, s), 8.00 (2H, br.s), 9.7 (1H, very br.s) ppm; and ¹³C-NMR: δ 8.44, 10.33, 12.81, 14.48, 17.94, 21.32, 30.43, 33.46, 96.32, 115.58, 127.04, 127.93, 139.31, 140.65, 143.70, 146.79, 149.78, 172.00 ppm.

Anal. Calcd. for C₃₅H₄₆N₄O₂ · ½ CH₃OH (570.8): C, 74.70; H, 8.48; N, 9.82.

Found: C, 75.08; H, 8.24; N, 10.01.

3,17-Diethyl-8,12-bis-[3-acetoxy-1(*S*)-methylpropyl]-2,7,13,18-tetramethyl-(21*H*,24*H*)-bilin-1,19-dione (5).

This verdin was synthesized from dipyrinone **8** in 69% yield. It had mp 204-207°C; ¹H-NMR: δ 1.22 (6H, t, J=7.5 Hz), 1.38 (6H, d, J=7.0 Hz), 1.81 (6H, s), 2.02 (6H, s), 2.01-2.10 (4H, m), 2.12 (6H, s), 2.51 (4H, q, J=7.5 Hz), 3.03-3.13 (2H, m), 3.87-3.96, 4.06-4.14 (4H, two m), 5.96 (2H, s), 6.85 (1H, s), 8.01 (2H, br.s), 10.0 (1H, very br.s) ppm; and ¹³C-NMR: δ 8.25, 10.24, 14.39, 17.85, 20.88, 21.37, 28.02, 35.83, 63.01, 95.93, 114.51, 127.18, 128.21, 139.77, 140.41, 142.02, 146.80, 150.11, 170.76, 172.01 ppm.

Anal. Calcd. for C₃₉H₅₀N₄O₆ (670.8): C, 69.82; H, 7.51; N, 8.35.

Found: C, 69.86; H, 7.49; N, 8.40.

3,17-Diethyl-8,12-bis-[3-acetamido-1(*S*)-methylpropyl]-2,7,13,18-tetramethyl-(21*H*,24*H*)-bilin-1,19-dione (6).

This verdin was synthesized from dipyrinone **9** in 56% yield. It had mp 221-223°C; ¹H-NMR: δ 1.20 (6H, t, J=7.6 Hz), 1.36 (6H, d, J=7.1 Hz), 1.80 (6H, s), 1.86 (6H, s), 1.88-1.96 (4H, m), 2.11 (6H, s), 2.51 (4H, q, J=7.6 Hz), 2.94-3.05 (4H, m), 3.29-3.38 (2H, m), 5.96 (2H, s), 6.41 (2H, br.s), 6.88 (1H, s), 8.33 (2H, br.s), 9.9 (1H, very br.s) ppm; and ¹³C-NMR: δ 8.27, 10.31, 14.42, 17.83, 21.73, 23.06, 29.81, 36.72, 38.89, 96.25, 114.92, 127.02, 128.19, 139.78, 140.32, 142.65, 146.89, 150.04, 170.41, 172.37 ppm.

Anal. Calcd. for C₃₉H₅₂N₆O₄ (668.8): C, 70.03; H, 7.84; N, 12.57.

Found: C, 69.64; H, 7.92; N, 12.38.

Mesobilirubin-XIII α analogs 1-3. General procedure. To a solution of 0.25 mmol of mesobiliverdin-XIII α analog **4-6** in 50 mL of dry deoxygenated THF, cooled in an ice bath, was added 945 mg (25 mmol) sodium borohydride followed by dropwise addition of 25 mL of dry CH₃OH over 15 min. under N₂. After stirring 30-45 min., the mixture was diluted with 150 mL of degassed ice water and acidified with 10% aq. HCl, added very slowly under N₂ while cooling with ice bath. The mixture was diluted further with 100 mL of H₂O, and the product was extracted into CHCl₃ (3 × 100 mL). The combined extracts were washed with H₂O (3 × 100 mL) until neutral, dried over anhydrous Na₂SO₄, and filtered. The solvent was removed under vacuum (<30°C), and the resulting crude product was purified by radial chromatography, eluting with 1.5-3% CH₃OH in CH₂Cl₂ for **1** and **2** or 3.5-5% CH₃OH in CH₂Cl₂ for **3**. After removing the solvent, the bright yellow fractions were recrystallized from a minimal volume of chloroform and methanol (added dropwise).

(-)-3,17-Diethyl-8,12-bis-[1(*S*)-methylpropyl]-2,7,13,18-tetramethyl-(10*H*,21*H*,23*H*,24*H*)-bilin-1,19-dione (1).

This rubin was obtained from verdin **4** in 89% yield. It had mp 246-249°C; [α]_D²⁰ -1490° (c 8.4 × 10⁻³, CHCl₃). ¹H-NMR: δ 0.83 (6H, t, J=7.3 Hz), 0.99 (6H, t, J=7.5 Hz), 1.30 (6H, d, J=7.1 Hz), 1.40 (6H, s), 1.62-1.72 (4H, m), 2.15 (6H, s), 2.31 (4H, q, J=7.5 Hz), 2.76-2.85 (2H, m), 4.12 (2H, s), 5.91 (2H, s), 10.17 (2H, br.s), 10.77 (2H, br.s) ppm; and ¹³C-NMR: δ 7.54, 11.08, 12.88, 14.74, 17.77, 20.69, 23.18, 29.60, 33.10, 99.98, 122.13, 123.26, 124.10, 124.17, 128.55, 131.01, 146.72, 174.06 ppm.

Anal. Calcd. for C₃₅H₄₈N₄O₂ · 1.5 CH₃OH (604.8): C, 72.48; H, 9.00; N, 9.26.

Found: C, 72.55; H, 8.31; N, 9.32.

(-)-3,17-Diethyl-8,12-bis-[3-acetoxy-1(*S*)-methylpropyl]-2,7,13,18-tetramethyl-(10*H*,21*H*,23*H*,24*H*)-bilin-1,19-dione (2).

This rubin was synthesized from verdin **5** in 67% yield. It had mp 251-253°C (decomp.); [α]_D²⁰ -1140° (c 4.4 × 10⁻³, CHCl₃); ¹H-NMR: δ 0.99 (6H, t, J=7.5 Hz), 1.35 (6H, d, J=7.1 Hz), 1.41 (6H, s), 1.94-2.03

(4H, m), 2.02 (6H, s), 2.16 (6H, s), 2.32 (4H, q, $J=7.5$ Hz), 3.02-3.11 (2H, m), 3.88-3.97, 4.00-4.08 (4H, two m), 4.10 (2H, s), 5.90 (2H, s), 10.20 (2H, br.s), 10.74 (2H, br.s) ppm; and ^{13}C -NMR: δ 7.55, 10.96, 14.72, 17.76, 20.98, 21.06, 22.98, 27.94, 35.12, 63.65, 99.81, 121.83, 122.74, 123.56, 124.41, 129.02, 130.44, 146.90, 170.96, 174.19 ppm.

Anal. Calcd. for $\text{C}_{39}\text{H}_{52}\text{N}_4\text{O}_6$ (672.8): C, 69.61; H, 7.79; N, 8.33.

Found: C, 69.44; H, 7.75; N, 8.25.

(-)-3,17-Diethyl-8,12-bis-[3-acetamido-1(*S*)-methylpropyl]-2,7,13,18-tetramethyl-(10*H*,21*H*,23*H*,24*H*)-bilin-1,19-dione (3). This rubin was synthesized from verdin **6** in 74% yield. It had mp 255-258°C (decomp.); $[\alpha]_{\text{D}}^{20} -1690^\circ$ (c 9.8×10^{-3} , CHCl_3); ^1H -NMR: δ 1.03 (6H, t, $J=7.6$ Hz), 1.33 (6H, d, $J=7.0$ Hz), 1.52 (6H, s), 1.73 (6H, s), 1.81-1.94 (4H, m), 2.14 (6H, s), 2.35 (4H, q, $J=7.6$ Hz), 2.90-3.00 (4H, m), 3.27-3.36 (2H, m), 4.12 (2H, s), 5.70 (2H, br.s), 5.96 (2H, s), 10.16 (2H, br.s), 10.35 (2H, br.s) ppm; and ^{13}C -NMR: δ 7.98, 11.05, 14.78, 17.80, 21.12, 22.89, 22.98, 29.87, 35.69, 38.93, 100.03, 121.86, 123.33, 123.88, 124.24, 129.99, 130.03, 147.24, 170.19, 174.35 ppm.

Anal. Calcd. for $\text{C}_{39}\text{H}_{54}\text{N}_6\text{O}_4$ (670.9): C, 69.82; H, 8.11; N, 12.53.

Found: C, 69.60; H, 7.83; N, 12.31.

Acknowledgment. We thank the National Institutes of Health (HD 17779) for generous support of this work. Dr. S.E. Boiadjev is on leave from the Institute of Organic Chemistry, Bulgarian Academy of Sciences. Mr. W.P. Pfeiffer gratefully acknowledges award of the Wilson Graduate Fellowship. We thank Mr. Lew Cary for invaluable assistance in obtaining NOE data for the ^1H -NMR spectra.

REFERENCES

- McDonagh, A.F. *Bile Pigments: Bilatrienes and 5,15-Biladienes*. In *The Porphyrins*; Dolphin, D., Ed.; Academic Press: New York, **1979**, 6, 293.
- Berk, P.D.; Noyer, C. *Seminars Liver Dis.*, **1994**, *14*, 323-394.
- Chowdury, J.R., Wolkoff, A.W., Chowdury, N.R., and Arias, I.M. "Hereditary Jaundice and Disorders of Bilirubin Metabolism" in *The Metabolic and Molecular Bases of Inherited Disease* (Scriver, C.R., Beaudet, A.L., Sly, W.S., and Valle, D., eds.) McGraw-Hill, Inc., New York, *Vol. II*, **1995**, chap. 67, 2161-2208.
- (a) Bonnett, R.; Davies, J.E.; Hursthouse, M.B.; Sheldrick, G.M. *Proc. R. Soc. London, Ser. B*, **1978**, *202*, 249-268.
(b) LeBas, G.; Allegret, A.; Mauguén, Y.; DeRango, C.; Bailly, M. *Acta Crystallogr., Sect. B*, **1980**, *B36*, 3007-3011.
(c) Mugnoli, A.; Manitto, P.; Monti, D. *Acta Crystallogr., Sect. C*, **1983**, *39*, 1287-1291.
- (a) Person, R.V.; Peterson, B.R.; Lightner, D.A. *J. Am. Chem. Soc.*, **1994**, *116*, 42-59.
(b) Lightner, D.A.; Person, R.V.; Peterson, B.R.; Puzicha, G.; Pu, Y.-M.; Boiadjev, S. *Bio-molecular Spectroscopy II* (Birge, R.R.; Nafie, L.A., eds.), Proc. SPIE *1432*, **1991**, 2-13.
(c) Person, R.V.; Boiadjev, S.E.; Peterson, B.R.; Puzicha, G.; Lightner, D.A. "4th International Conference on Circular Dichroism," Sept. 9-13, 1991, Bochum, FRG, pp 55-74.

6. Shelver, W.H.; Rosenberg, H.; Shelver, W.H. *Intl. J. Quantum Chem.*, **1992**, *44*, 141-163.
7. (a) Kaplan, D.; Navon, G. *Israel J. Chem.* **1983**, *23*, 177-186.
(b) Kaplan, D.; Navon, G. *J. Chem. Soc., Perkin Trans 2* **1981**, 1374-1383.
(c) Navon, G.; Frank, S.; Kaplan, D. *J. Chem. Soc., Perkin Trans. 2* **1984**, 1145-1149.
8. (a) Boiadjiev, S.E.; Person, R.V.; Puzicha, G.; Knobler, C.; Maverick, E.; Trueblood, K.N.; Lightner, D.A. *J. Am. Chem. Soc.* **1992**, *114*, 10123-10133.
(b) Puzicha, G.; Pu, Y-M.; Lightner, D.A. *J. Am. Chem. Soc.* **1991**, *113*, 3583-3592.
9. Nogales, D.; Lightner, D.A. *J. Biol. Chem.* **1995**, *270*, 73-77.
10. Boiadjiev, S.E.; Lightner, D.A. *Tetrahedron: Asymmetry*, **1996**, *7*, 1309-1322.
11. Lightner, D.A.; Gawroński, J.K.; Wijekoon, W.M.D. *J. Am. Chem. Soc.* **1987**, *109*, 6354-6362.
12. Lightner, D.A.; Wijekoon, W.M.D., Zhang, M.H. *J. Biol Chem.* **1988**, *263*, 16669-16676.
13. Blauer, G. *Israel J. Chem.* **1983**, *23*, 201-209.
14. (a) Boiadjiev, S.E.; Lightner, D.A. *Synlett.* **1994**, 777-785.
(b) Shrout, D.P.; Puzicha, G.; Lightner, D.A. *Synthesis* **1992**, 328-332.
15. Boiadjiev, S.E.; Anstine, D.T.; Lightner, D.A. *J. Am. Chem. Soc.* **1995**, *117*, 8727-8736.
16. Shrout, D.P.; Lightner, D.A. *Synthesis* **1990**, 1062-1065.
17. Boiadjiev, S.E.; Anstine, D.T.; Maverick, E.; Lightner, D.A. *Tetrahedron: Asymmetry* **1995**, *6*, 2253-70.
18. Harada, N.; Nakanishi, K. *Circular Dichroic Spectroscopy - Exciton Coupling in Organic Stereochemistry*; University Science Books: Mill Valley, CA, 1983.
19. For leading references, see: Falk, H. *The Chemistry of Linear Oligopyrroles and Bile Pigments*; Springer Verlag: NY, **1989**.
20. Nogales, D.F.; Ma, J-S.; Lightner, D.A. *Tetrahedron* **1993**, *49*, 2361-2372.
21. Dörner, T.; Knipp, B.; Lightner, D.A. *Tetrahedron* **1997**, *53*, 2697-2716.
22. Perrin, D.D.; Armarego, W.L.F. *Purification of Laboratory Chemicals*, 3rd Ed., Pergamon Press, England, 1988.

(Received in USA 20 June 1997; revised 19 August 1997; accepted 22 August 1997)